Dalton Transactions

Accepted Manuscript

ROYAL SOCIETY OF CHEMISTRY

www.rsc.org/dalton

Journal Name

RSCPublishing

ARTICLE

On the origin of stereocontrol in the directed ortho lithiation of phosphinimidic amides. NMR spectroscopic and computational study of the structure of *N*-lithiated (*R*)-$Ph_2P(=NCO_2Me)NHCH(Me)Ph$

Cite this: DOI: 10.1039/x0xx00000x

Received ooth January 2012,
Accepted ooth January 2012

DOI: 10.1039/x0xx00000x

www.rsc.org/

María Casimiro,[a] Jesús García López,[a] María José Iglesias,[a] and Fernando López Ortiz*[a]

A multinuclear magnetic resonance (^1H, ^7Li, ^{13}C, ^{15}N, ^{31}P) and DFT computational study at the M06-2X(SMD,THF)/6-311+G(d,p)//B3LYP/6-31G(d) level of the structure of a *N*-lithiated phosphinimidic amide (*R*)-$Ph_2P(=NCO_2Me)NHCH(Me)Ph$ **13** has been performed. In THF solution it exists as an equilibrium mixture of monomers and dimers. The monomers consist of a six-membered ring formed by coordination of the lithium atom with the deprotonated nitrogen and the oxygen atom of the carbonyl group. This coordination mode is in contrast to the standard *N,N*-chelation observed in *N*-lithiated *N,N'*-bis(trimethylsilyl)phosphinimidic amides. The calculations showed that the metallacycle adopts a twist-boat conformation and that the lithium atom is in a tetrahedral environment involving *O,N*-chelation by the ligand and coordination to two/one THF molecules in the monomer/dimer. Dimerization takes place through O-Li bridges. For all species two series of isomers have been identified originated by restricted rotation of the methoxy group and ring inversion. The twist-boat conformational interconversion seems to be operating for explaining the pattern of signals observed in the ^7Li and ^{31}P NMR spectra. The structure found for the most stable dimer is analogous to the molecular structure reported for a related C_α-lithiated phosphazene **20**. The structural study revealed that the chiral side-arm of the *N*-lithiated species is oriented to the outer face of the *pro-S P*-phenyl ring, which shows one *ortho*-proton very close to the nitrogen atom of the carbamate moiety. In this conformation, proton abstraction of that proton by a base is highly favoured, in agreement with the experimental results.

Introduction

Phosphinimidic amides are important ligands in coordination chemistry and catalysis.[1] The NPN framework of the deprotonated species $[R^1{}_2P(NR^2)_2]^-$ is an excellent coordination group for the stabilization of a wide variety of complexes of main-group,[2] d-block[3] and rare-earth elements.[4] The most studied applications of these complexes are as precatalysts in alkene cyclopropanation[5] and in oligomerization[6] and polimerization[7] reactions. More recently, copper and nickel complexes based on the NPN moiety have been applied as efficient catalysts in alkene aziridination[8] and Kumada cross-coupling reactions.[9]

Generally, phosphinimidic amide complexes are prepared via salt-methatesis using the lithiated species as ligand transfer reagents.[1a,b] As a rule, *N*-lithiated phosphinimidic amides act as chelating monoanionic ligands leading to the formation of four-membered metallacycles **1** (Fig. 1). Chelation to give larger metallacycles is possible in phosphinimidic amides in which the negative charge of the $[N\text{-}P\text{-}N]^-$ skeleton may be delocalized through the *N*-substituents. Thus, complex **2** exists as a six-membered ring *N,S*-chelate due to the binding of the negatively charged nitrogen and the sulfur of the N-P=N-P=S system to the cobalt cation.[10] The presence of additional coordination sites in the substituents of the phosphinimidic amide not involved in charge delocalization provides alternative possibilities of chelation. The pyridyl ring of complexes **3**[11] and **4**[12] determines that the anion act as a tridentate and tetradentate ligand, respectively. Interestingly, *N,N'*-chelation in **3** and **4** takes place with one nitrogen of the $[N\text{-}P\text{-}N]^-$ backbone and the nitrogen of a pyridine ring.

Unusual coordination modes of phosphinimidic amide anions having their roots in steric interactions are also known. The potassium complex **5** is a remarkable example. The molecular structure shows no N···K contacts. The formation of a four-membered ring through *N,N'*-chelation is hindered by the steric strain arising from the bulky 2,6-$^i Pr_2C_6H_3$ (Dip) groups. As a consequence, only arene···K coordination is observed.[3f] This is in contrast to the molecular structure of the only other phosphinimidic amide potassium complex previously reported, $\{K[Ph_2P(NSiMe_3)_2(THF)_4\}$, where the ligand features the usual *N,N'*-chelate behavior.[2b] One example of $[N\text{-}P\text{-}N]^-$ bridging rather than chelation coordination has been reported. The reaction of $\{Li[Ph_2P(=NSiMe_3)_2]\}$ with

$CuCl$[13] or $CuBr(SMe)_2$[8] affords the dinuclear complex **6**. The structure of **6** revealed that two NPN ligands are connected through copper bridges furnishing an eight-membered metallacycle.[14]

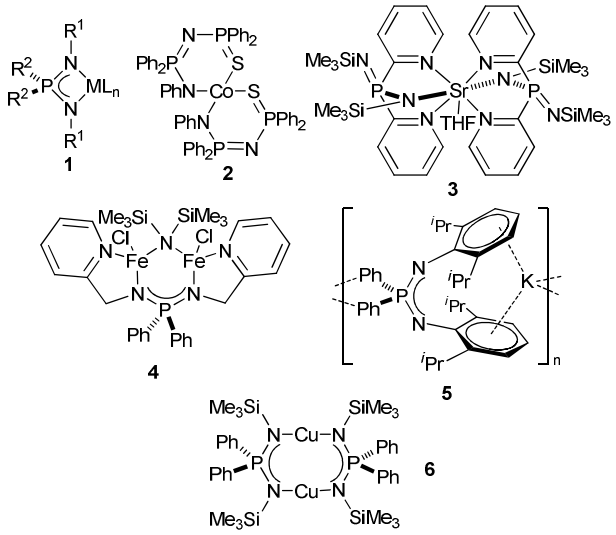

Figure 1. Representative examples of $[N\text{-}P\text{-}N]^-$ coordination modes.

Concerning the parent lithiated species, a number of X-ray crystal structures of monolithiated phosphinimidic amides have been reported (Fig. 2).[15] Complexes **7** – **11** consist of monomers where the $[N\text{-}P\text{-}N]^-$ anion is chelating the lithium cation, giving rise to a four-membered ring, and the metal completes the tetrahedral coordination by binding to two additional monodentated ligands (THF or pyridine). The solid-state structure of the dilithium bis(phosphinimidic amide) **12** has been also described.[7c] In this complex the phosphinimidic amide moieties are built on a *rac-trans*-1,2-diaminocyclo-hexane scaffold. This arrangement allows for an interaction between the two Li[N-P-N] fragments, resulting in the formation of an eight-membered metallacycle in which the lithium ions are bridging the $[N\text{-}P\text{-}N]^-$ anions.

As part of our ongoing research on lithiations directed by *P*-based functional groups,[16] we have reported the efficient synthesis of *ortho*-functionalized (S_P,R_C)-phosphinimidic amides **14** (Scheme 1).[17] The process involves the diastereose-lective formation of the N,C_{ortho}-dilithiated species **II** by treatment of the chiral phosphinimidic amide **13** with 3 equiv of *t*-BuLi in THF at -90 ºC followed by electrophilic quench.[18] Subsequent functional group transformations showed that the method represents a valuable route for accessing to a wide variety of enantiopure functionalized *P*-stereogenic compounds (e.g., **14** – **17**).[19]

The high diastereoselectivity observed in the formation of dianion **II** implies that the structure of the precursor monolithiated phosphinimidic amide **I** favors the almost exclusive abstraction of one ortho proton of the *pro-S* phenyl ring by the organolithium base (Scheme 1). Curiously, Wang and co-workers have recently reported that the monolithiation with ^{n}BuLi of a compound analogous to **13**, the *N*-*tert*-butyl-*P*,*P*-diphenyl-*N'*-(quinolin-8-yl)phosphinimidic amide, takes place at the ortho position of a *P*-phenyl ring rather than at the NH.[18e]

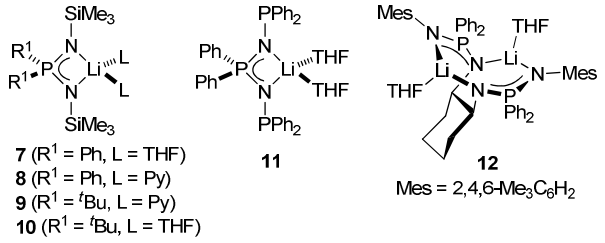

Figure 2. Molecular structures of lithiated phosphinimidic amides.

To the best of our knowledge, the structure of lithiated phosphinimidic amides in solution remains essentially unknown. Cryoscopic determinations on benzene solutions of complexes **7** and {Li[^{t}Bu$_2$P(=NMe)NH]} suggested the existence of dimers[20] and trimers,[21] respectively. NMR spectra in C_6D_6 have been measured at room temperature in a few cases (**7**, **11**, **12**). They only provide information about an average structure.

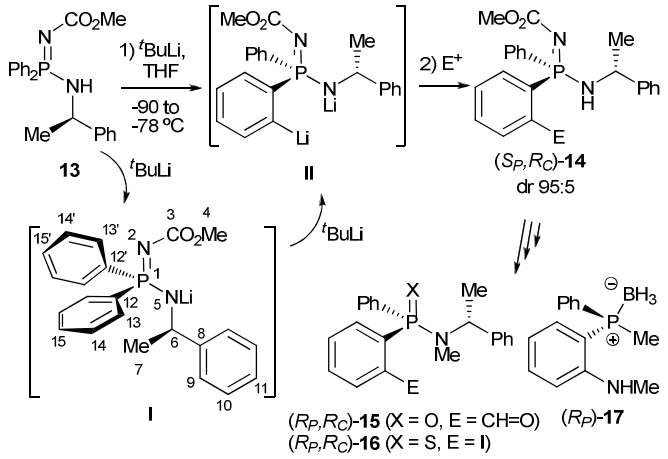

Scheme 1. Synthesis of *P*-stereogenic compounds through diastereoselective *o*-deprotonation of diastereotopic phenyl groups of phosphinimidic amides.

In order to get an insight into the origin of the diastereoselectiviy observed in the formation of dianion **II** we have carried out a multinuclear magnetic resonance (^{1}H, ^{7}Li, ^{13}C, ^{15}N, ^{31}P) and computational study of the structure of the monolithiated species **I**. The results obtained are reported here.

Results and discussion

NMR spectroscopic studies

NMR samples were prepared in accordance with the lithiation procedure previously optimized in the laboratory for the N,C_{ortho}-dilithiation of **13**, except for the amount of base. A solution of phosphinimidic amide **13** in THF (or THF-d_8) was treated with 1 equiv of *t*-BuLi at -78 ºC during one hour. Then, 0.5 mL of the reaction mixture were transferred under N_2 atmosphere to a 5 mm NMR tube placed into a bath at -78 ºC. Right after the preparation, the sample was placed into the magnet previously cooled to the working temperature. ^{7}Li and ^{31}P NMR measured in the temperature range -70 ºC to -20 ºC revealed that mono-deprotonation of **13** proceeded almost quantitatively. The ^{7}Li-NMR spectra of **I** show a single signal at δ 0.95 ppm. Concerning the ^{31}P NMR spectra, they consist of a signal at δ 19 ppm together with less than 5% of starting

material. This means that the phosphinimidic amide **13** undergoes a shielding of 2 ppm upon monolithiation.

Deprotonation exclusively at the N-H position[22] of **13** was evidenced in the ^{1}H-NMR spectrum acquired at -20 ºC by the disappearance of the NH signal, as well as the corresponding vicinal coupling with the adjacent methine proton H6 (δ 4.08 ppm, dq $^{3}J_{PH}$ 20.8, $^{3}J_{HH}$ 6.4 Hz) (Fig S1, supporting information). Furthermore, the diastereotopic *P*-phenyl rings show the anticipated pattern for monosubstituted phenyl groups. The assignment of the ^{1}H signals of all aromatic protons of **I** could be readily accomplished (Table S1) based on the analysis of the COSY45 NMR spectrum (Fig S2). The ^{13}C- and dept135 NMR spectra measured at -20 ºC proved that species **I** retains the same hydrocarbon skeleton as that of **13** (Fig S3). Interestingly, carbons C4 (δ 53.44 ppm), C6 (δ 55.35 ppm) and C7 (d, δ 28.64 ppm, $^{3}J_{PC}$ 8.7 Hz) appear as broad signals, which suggests that they may participate in some dynamic process. Experimental confirmation about the site of lithiation in **I** was obtained by quenching the sample with CD_3OD. The ^{1}H-, ^{13}C- and ^{31}P-NMR spectra of the deuterated sample measured at room temperature were identical to those of **13**, except for the absence in the ^{1}H spectrum of the NH signal and the respective $^{3}J_{HH}$ coupling (Fig S4).

Once established that **I** is a *N*-lithiated species, we sought to identify the coordination mode of the organic ligand. As pointed above, lithiated phosphinimidic amides behave as *N,N*-chelate ligands towards lithium ions (Fig 2). In species **I**, delocalization of the negative charge through the CO_2Me group conjugated with the P=N linkage may lead to the formation of a six-membered *O,N*-chelate. This fundamental dichotomy could be solved by analyzing the heteronuclear correlations of the nitrogen atoms of **13** and **I**. The 2D ^{31}P,^{15}N{^{1}H}-HMQC spectrum[23] of **13** afforded the expected correlations of the phosphorus nucleus with N5 (s, δ -321.3 ppm) and N2 (d, δ -280.6 ppm, $^{1}J_{PN}$ 35 Hz) (Fig 3a). These assignments are supported by the similarity of the chemical shift of N2 with those reported for related phosphazenes (range of -244.4 to -315.6 ppm).[24] Moreover, N5 was unequivocally identified through the correlation with the NH proton in the ^{1}H,^{15}N HMQC experiment (Fig S5). The analogous experiment performed with the lithiated species **I** (Fig 3b) showed that N2 (δ -256.5 ppm) undergoes a large shielding, whereas N5 (δ -320.1 ppm) is almost unaffected as compared with the parent compound **13**.[25] The magnitude of the ^{31}P,^{15}N coupling constants in **I** are more revealing. The values obtained for N2 ($^{1}J_{PN}$ 16 Hz) and N5 ($^{1}J_{PN}$ 36 Hz) involve a large decrease/increase of $^{1}J_{PN}$ for N2/N5 with respect to **13**. These differences of $^{1}J_{PN}$ of **I** vs. **13** can be explained by a lengthening/shortening of the P-N2/P-N5 bond distance in the lithiated species **I**, in agreement with the experimental observations for lithiated phosphinimidic amides. Compounds **7**-**12** show equal P-N bond distances within the ring of a bond order of ca. 1.5, average between a single and a double phosphorus-nitrogen bond.[7c,15d]

The definite evidence about the coordination mode of the ligand in **I** was provided by a ^{7}Li,^{15}N{^{1}H}-HMQC experiment.[26] The spectrum was acquired at -100 ºC on a 0.3 M sample (Fig 3c). At this very low temperature two ^{7}Li/^{15}N correlations were detected. The origin of these two signals will be made clear later, in connection with the aggregation studies. The important point here is that the ^{15}N chemical shifts observed correspond to N5, *i.e*, only N5 is scalarly coupled to a lithium nucleus. This indicates that the delocalized bonding scheme of the [N-P-N]$^{-}$ moiety is extended to the C=O linkage of the CO_2Me group and, therefore, species **I** exists in THF solution as a six-membered metallacycle formed by *O,N*-chelation of the lithium cation (Scheme 2).[27] Most probably, the lithium ion completes its coordination sphere by binding to THF molecules. Significantly, the same structural features found in **I** have been reported for the C_α-lithiated phosphazene **19** and its dimer **20** formed in the reaction of phosphazene **18** with *n*-BuLi in THF at -30 ºC.[28]

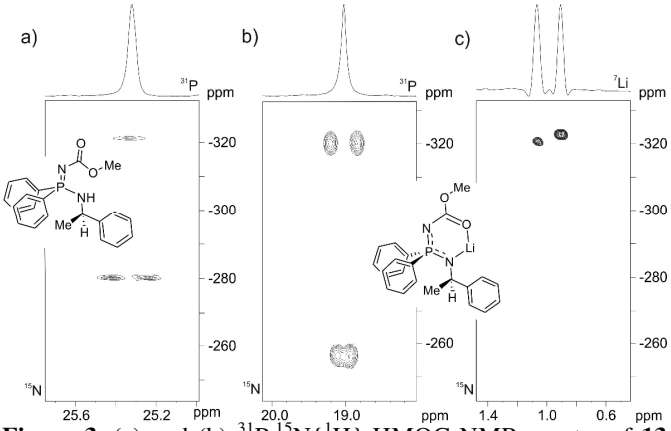

Figure 3. (a) and (b) ^{31}P,^{15}N{^{1}H}-HMQC NMR spectra of **13** (0.3 M, $CDCl_3$) and **I** (0.3 M, THF-d_8), respectively, measured at -20 ºC. (c) ^{7}Li,^{15}N HMQC NMR spectrum of **I** (0.3 M, THF-d_8) measured at -100 ºC.

As it has been mentioned above, the conformation adopted by the monolithiated intermediate **I** in solution determines the diastereoselectivity of the subsequent *ortho*-lithiation step (Scheme 1). Following this line of thought, a 2D ROESY experiment was performed at -20 ºC. The spectrum showed NOEs between H6 (δ 4.08 ppm) and H7 (δ 1.32 ppm) with the ortho protons of only one *P*-phenyl ring H13' (δ 7.79 ppm) (Figs 4 and S6). This means that the chiral side-arm is close to the outer face of only one *P*-phenyl ring.

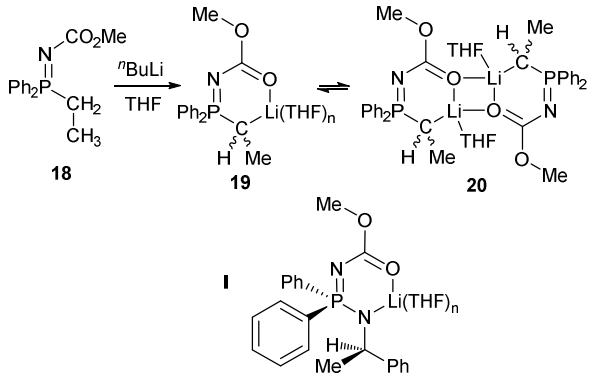

Scheme 2. Structural similarity between the products of C_α-lithiation of phosphazene **18** and the *N*-lithiated phosphinimidic amide **I**.

Concerning the *ortho*-lithiation, it is tempting to say that this proximity blocks the access of the incoming base to that phenyl ring and, therefore, *ortho*-lithiation must be directed preferably to the *P*-phenyl that is not in the neighborhood of the chiral auxiliary. However, an alternative scenario is also possible. The spatial proximity detected in the ROESY spectrum may promote the approach of the *P*-phenyl group allocated on the same side of the chiral auxiliary to the

phosphinimidic moiety, so that the corresponding ortho protons will be in a more favorable position for abstraction by the base.

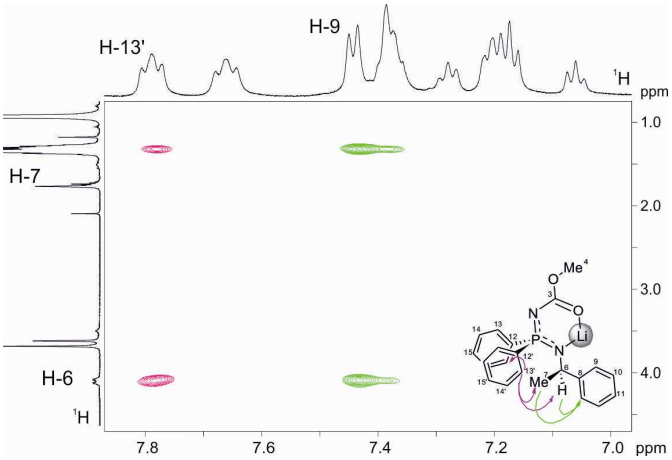

Figure 4. Expansion of the 2D ROESY spectrum of **I** measured in THF-d_8 at -20 ºC showing key NOE correlations. The methyl protons H7 are buried into the signal of the solvent of the *t*-BuLi solution used.

Except for the ^{7}Li,^{15}N correlation acquired at -100 ºC (Fig 3c), the NMR spectra analysed thus far were measured at -20 ºC and showed the presence of a single species. Changes in the NMR spectra of organolithium compounds as a function of the temperature are commonly due to the existence of equilibria among different aggregates.[29] In order to shed light on the aggregation state of **I** a variable temperature and concentration NMR study was undertaken. Firstly, we investigated the effect of the temperature on a 0.05 M sample, which represents the concentration used in the laboratory scale reactions.[17] Lowering gradually the temperature causes a progressive broadening of the ^{1}H NMR signals and, finally, their splitting into two sets of very broad signals at temperatures below -80 ºC (Fig S7). Like protons, the ^{31}P signal of **I** begins to split at -80 ºC (Fig S8) and at -120 ºC the spectrum consist of six sharp singlets (labelled as **13**, **13'**, **Mα-Mδ**, Table 1, Fig 5a) together with a set of much less intense and broad signals (labelled as **Dα-Dζ**, Table 1, Fig 5a). We have chosen to use Greek letters to distinguish the subtypes of aggregates to avoid the mixing of the labels between NMR detected species and computed structures (see computational section).

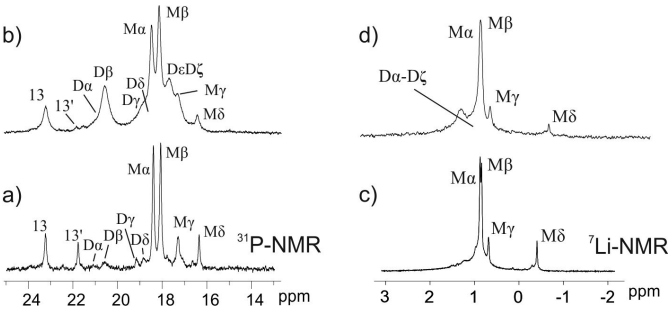

Figure 5. (a)/(b) ^{31}P and (c)/(d) ^{7}Li NMR spectra of a (a)/(c) 0.05 M and (b)/(d) 0.3 M sample of **I** in THF-d_8 measured at -120 ºC.

Signals **13** and **13'** proceed from the starting material (incomplete NH deprotonation). The two ^{31}P observed are assigned to the two rotamers generated by the restricted rotation of the MeO group with respect to the C=O linkage.[30] Species **M/D** might be considered as different aggregates, a common feature of organolithium compounds in solution.

Table 1. ^{31}P and ^{7}Li chemical shifts (ppm) of a 0.05 M sample of **I** in THF-d_8 measured at -120 ºC.

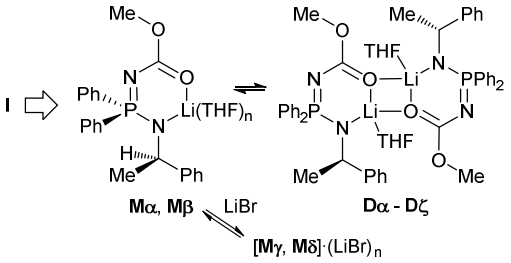

Nucleus	Mα	Mβ	Mγ	Mδ		
^{31}P	18.40	18.07	17.29	16.35		
^{7}Li	0.87	0.84	0.69	-0.41		
	Dα	**Dβ**	**Dγ**	**Dδ**	**Dε**	**Dζ**
^{31}P	21.09	20.55	19.15	18.85	17.80	17.50

As for **13/13'**, species **M/D** may also participate in dynamic processes regarding the rotation of the OMe group. To validate this hypothesis, a variable concentration ^{31}P NMR study was achieved (range of concentrations of 0.05 M to 0.3 M, Fig. S9). Spectra corresponding to the most diluted/concentrated sample are given in Figs 5a/5b. This study showed a random change of the integrals of signals **Mγ** and **Mδ**, whereas the integrals of signals **Dα-Dζ** increased with increasing concentration at expenses of signals **Mα** and **Mβ**. A plot of log[**Dα-Dζ**] vs. log[**Mα-Mβ**] afforded a straight line of a slope of 1.6, indicating that species **Dα-Dζ** and **Mα-Mβ** are different aggregates that correspond reasonably well to an equilibrium monomer-dimer (Fig S10).[31] Signals **Mγ** and **Mδ** are tentatively assigned as mixed aggregates formed between monomers **Mα-Mβ** and the LiBr present in the organolithium base (they persist in the most diluted sample).[32] Mixed aggregates of *N*-lithium phosphazenes and lithium bromide are known in the literature.[33] Support for the assignments made was obtained based on ^{31}P{^{1}H}-EXSY experiments on the 0.3 M sample at -115 ºC (Figs 6 and S12). The patterns of signal/cross peaks observed suggests that (*i*) the ^{31}P nuclei of dimers are not equivalents, (*ii*) signals **Dα** to **Dδ** represent the half part of genuine dimers, with the signal from the other half part appearing at δ 17.4 ppm (for **Dα**) and δ 17.8 ppm (for **Dβ-Dδ**), (*iii*) dimer **Dβ** is in equilibrium (exchange) with dimers **Dγ-Dδ** and monomer **Mβ**, which in turn is in equilibrium with **Mα**, and (*iv*) both monomers are in exchange with the mixed aggregate **Mδ**.

The ^{7}Li NMR spectrum of the most diluted sample showed similar features to those found for ^{31}P (Fig 5c, see also spectra for the range of concentrations of 0.05 M to 0.3 M, Fig. S13). The signals of monomers **Mα-Mδ** are easily recognised. However, the much less intense and broad lithium signals of dimers **Dα-Dζ** are only barely distinguishable at the base of **Mα-Mβ**. This situation does not improve appreciably at the highest concentration used (Fig 5d). Only one broad signal of the dimeric species is resolved. The ^{7}Li,^{31}P{^{1}H}-HMQC spectrum[34] furnished the ^{7}Li,^{31}P connectivity for monomers **Mα** and **Mβ** (Fig S14). A third correlation arising from **Dα** or **Dβ**

was also detected. It can't be unequivocally assigned due to the overlap of the ^{31}P and ^{7}Li signals.

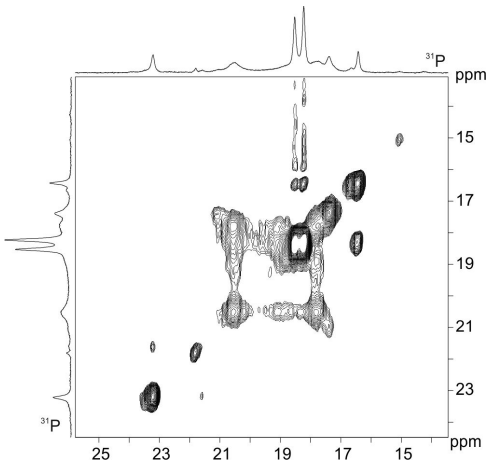

Figure 6. $^{31}P\{^{1}H\}$-EXSY spectrum (mixing time of 100 ms) of a 0.3 M sample of **I** in THF-d_8 measured at -115 ºC.

Analogously to **13/13'**, the duplicity of signals for a monomeric species, **Mα** and **Mβ**, can be explained by the existence of syn and anti isomers of the methyl carbamate moiety.[30] This type of conformational equilibrium has also been found in the lithiated phosphazene **19**[28] and, most probably, will be also present in dimers **Dα**-**Dζ**. Based on the similarity between lithiated phosphazene **19** and species **I**, it is suggested that dimerization takes place by assembling monomeric units through O–Li–O bridges, resulting in structures analogue to **20** (Table 1).[35] The anisochrony of the ^{31}P nuclei in dimers **Dα**-**Dζ** might be due to the lack of symmetry produced by the conformations adopted by the four- and six-membered metallacycles[36] and/or the rotamers generated by the restricted rotation of the MeO group.

To summarize this section, monolithiated phosphinimidic amide **I** exists in THF solution as an equilibrium mixture of monomers **Mα**-**Mβ** and dimers **Dα**-**Dζ**. The monomers consists of six-membered *O*,*N*-chelates with the lithium ion. They self-assemble through Li_2O_2 cores to give dimers **Dα**-**Dζ**. Both monomers and dimers are involved in conformational equilibria related to the flexibility of the metallacycles and/or the rotation of the methoxy group.

Computational studies

To resolve the ambiguities remaining about the structures of monomers and dimers, a DFT computational study at the M06-2X(SMD,THF)/6-311+G(d,p)//B3LYP/6-31G(d) level of theory was carried out. Single point calculations have been performed for all structures. The effect of the solvent has been included using the SMD solvent model.[37] All energies were calculated at a temperature of 183 K. The first issue addressed was the origin of conformational equilibria between monomers. Given that the lithium ion of organolithium compounds tends to reach tetracoordination,[38] the relative energy of the *O*,*N*-chelates in which the lithium ion is solvated by THF molecules, $(THF)_n$ where n = 0, 1 and 2 were calculated. The calculations revealed that monomeric *O*,*N*-chelates may exists as two families of isomers depending on the conformation of the six-membered matallacycle and the relative orientation of the methoxy group (Table S2). They are labelled as **M1a**, **M1b**, **M2a** and **M2b**, plus the corresponding solvation molecules. The letters "a"/"b" are used to indicate the syn/anti orientation of the MeO group with respect to the nitrogen atom of the carbamate moiety. The numbers "1"/"2" refer to the conformation of the six-membered rings, twist-boat in both cases. In structures "1" the methine proton of the stereogenic carbon is quasi perpendicular to the pseudo-equatorial *P*-phenyl ring, whereas in isomers "2", this C-H bond is located almost on the bisection of the Ph-P-Ph angle. This alignment leads to a face-to-face orientation of the pseudo-equatorial *P*-phenyl with the phenyl ring of the chiral arm.[39]

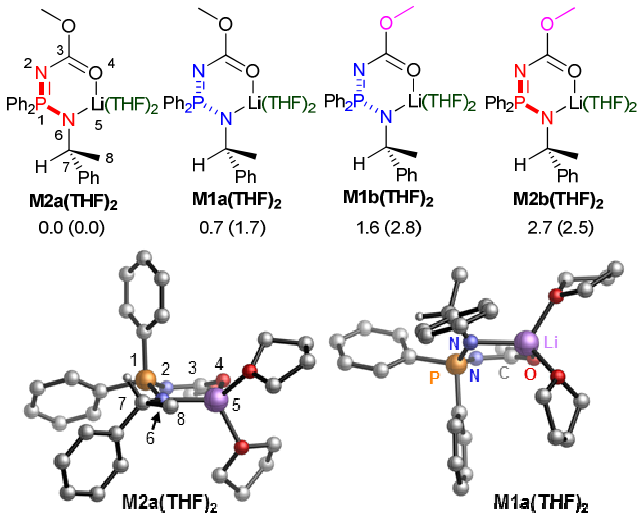

Figure 7. Structure of the four most stable monomeric *O*,*N*-chelates and 3D representation of isomers **M1a(THF)$_2$** and **M2a(THF)$_2$**. Hydrogen atoms have been omitted for clarity. Free energies and enthalpies (in parentheses) are given in kcal/mol with respect to **M2a(THF)$_2$**.

The most stable structures are the dissolvated species having the methoxy group oriented syn to the adjacent nitrogen **M1a(THF)$_2$** and **M2a(THF)$_2$**, with the latter being 0.7 kcal/mol more stable than the **M1a(THF)$_2$** isomer. The corresponding methoxy rotamers are destabilized by 1.6 and 2.7 kcal/mol for **M1b(THF)$_2$** and **M2b(THF)$_2$**, respectively (Fig 7). These differences of stability suggest that the two monomeric species observed in the ^{31}P NMR spectra at very low temperatures most probably arise from the two conformations adopted by the metallacycle. Although the energy barrier of ring inversion of free THF is too low (ca. 4 kcal/mol)[40] to be detected in the low temperature NMR measurements, it is not possible to discard the fluxionallity of THF bound to the lithium cation as responsible of the dynamic behavior observed for monomers.

Bond distances in the P1-N2-C3-O4 framework (Table 2) of **M1a(THF)$_2$** and **M2a(THF)$_2$** are very similar to those found in the dimeric structure of C_α-lithiated phosphazene **20** (e.g., 1.634(3) Å and 1.245(3) Å for the P-N and C-O bonds, respectively).[33] The P-N bond lengths are closer to the single bond of neutral phosphinimidic amides (average of 1.654 Å) than to the P=N linkage (average of 1.533 Å).[7c,15d,41] Significantly, the P1-N6 bond is shorter than the P1-N2 distance. This result supports the explanation given above regarding the differences of $^{1}J_{PN}$ observed between **13** and the *N*-lithiated derivative **I** (see Fig. 3a,b). The N6-Li5 and O4-Li5 bond distances are similar to those found in lithium complexes **7**-**12**,[7c,15] and **20**, respectively. The lithiated nitrogen N6 is

notably pyramidalized. Although the sum of bond angles for N6 is close to 360º in both isomers, there is a large deviation from a trigonal configuration due to the small P1-N6-Li5 bond angle (106.63º - 108.7º). Furthermore, the distances from N6 to the centroid of the plane comprising the P1, O4 and C7 atoms of 0.321 Å (**M1a(THF)$_2$**) and 0.344 Å (**M2a(THF)$_2$**) are consistent with a significant pyramidalization of N6.[42] The twist-boat conformational relationship between **M1a(THF)$_2$** and **M2a(THF)$_2$** is shown by the magnitude of the torsion angles C3-N2-P1-N6 and P1-N6-C7-C8. In both conformations, the chiral auxiliary blocks the outer face of the *pro-S P*-phenyl ring. Interestingly, one of the THF molecules coordinated to the metal is also close to the outer face of the *pro-R P*-phenyl ring.

Table 2. Selected distances (Å) and angles (º) of **M1a(THF)$_2$** and **M2a(THF)$_2$**.

Parameter	**M1a(THF)$_2$**	**M2a(THF)$_2$**
P1-N2	1.6448	1.6550
P1-N6	1.6169	1.6107
N2-C3	1.3271	1.3274
C3-O4	1.2581	1.2603
O4-Li5	1.8946	1.8954
Li5-N6	2.0292	2.054
P1-N6-Li5	108.7	106.63
P1-N6-C7	121.61	123.62
C7-N6-Li5	124.44	124.21
C3-N2-P1-N6	-48.34	42.53
C3-O4-Li5-N6	-31.41	-31.11
P1-N6-C7-C8	-152.93	-96.69

To complete the structural study of the monomeric species, the structures of the hypothetical *N,N*-chelates of lithiated phosphinimidic amide **13** solvated by two THF molecules were computed. Two energy minima **M3a(THF)$_2$** and **M3b(THF)$_2$** containing Li-N-P-N four-membered rings were found. They are isomers due to the restricted rotation around the C-N bond (Fig 8).[43] The geometrical parameters of **M3a(THF)$_2$** and **M3b(THF)$_2$** are very similar to those reported for the molecular structures of complexes **7** – **11**.[15] In this case, the structures lack symmetry and, therefore, two different P-N bond distances are observed (Table S3). **M3a(THF)$_2$** with the C=O linkage oriented syn to the phosphorus atom proved to be 1.5 kcal/mol more stable than the anti isomer **M3b(THF)$_2$**. The important point is that these *N,N*-chelates are remarkably destabilized as compared with the six-membered *O,N*-chelates **M1a(THF)$_2$** and **M2a(THF)$_2$** ($\Delta G^{183} \geq 2.8$ kcal/mol).

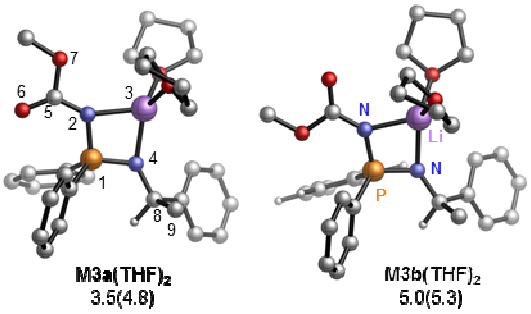

Figure 8. Structures of **M3a(THF)$_2$** and **M3b(THF)$_2$**. Hydrogen atoms have been omitted for clarity. Free energies and enthalpies (in parentheses) are given in kcal/mol with respect to **M2a(THF)$_2$**.

The computational study shows that the most favourable structures of monomers are two conformers of six-membered metallacycles, **M1a(THF)$_2$** and **M2a(THF)$_2$**, formed by *O,N*-coordination of the ligand to the lithium cation via the oxygen of the carbonyl group and the deprotonated nitrogen atoms. The metal achieves four-coordination by binding to two THF molecules. In these isomers access to the phenyl ring that undergoes selective proton abstraction seems to be hindered by the chiral side-arm. These results are in excellent agreement with the structural assignments made based on the NMR analysis. How, then, can be understood the high diastereoselectivity with which the *ortho*-lithiation of species **I** takes place (Scheme 1)?

As pointed above, the access to the outer faces of the *P*-phenyl rings is sterically hindered by either the chiral auxiliary or one THF molecule. According to the CIPE model[44] the approach of the base might be directed by the lone pair of N2. It occurs that the distance of the *pro-S* ortho proton to N2 is much shorter than that of the *pro-R* (2.503 Å *vs* 3.261 Å for **M2a(THF)$_2$** and 2.512 Å *vs* 2.660 Å for **M1a(THF)$_2$**). This proximity explains the highly preferred deprotonation of the *pro-S P*-phenyl ring. Therefore, the role of the chiral auxiliary appears to be that of favouring a disposition of the *pro-S P*-phenyl ring that brings one ortho proton in close proximity to the non-deprotonated nitrogen atom. A detailed study of the ortho-lithiation of **M2a(THF)$_2$/M1a(THF)$_2$** and the structure of the *N,C$_{ortho}$*-dianion **II** is currently in progress.

Aggregation of monomeric species **I** into dimers may originate a large number of structures. In compounds involving O-Li and N-Li bonds, dimerization via O-Li and N-Li bridges is feasible. The resulting dimers will show the same conformational behaviour found in the parent monomers and could exhibit different degree of lithium solvation by THF. All these possibilities have been evaluated. Firstly, O-Li *vs.* N-Li dimerization was investigated using unsolvated species as model dimers (Tables S4 and S5). The structures obtained were identified according to the same labelling scheme used for monomers as **Dna-c**, n = 1 to 3 are associated to the conformers of the six-membered rings in dimers with an O_2Li_2 core and n = 4 and 5 applies to N_2Li_2 dimers; a-c indicate the three different orientations of the MeO group (a: syn/syn, b: anti/anti and c: syn/anti with respect to the nitrogen atom).
Dimers consisting of mixed conformers of the six-membered *O,N*-chelates **D3a**, and **D5a** proved to be the most stable species for O-Li and N-Li bridged systems, respectively (Fig 9). Dimerization with formation of O-Li-O-Li four-membered rings is largely favoured ($\Delta G^{183} = 3.7$ kcal/mol).

Additional stabilization was provided by including explicit THF solvation of the metal ions. We have evaluated the effect of saturating the tetracoordination of either one or both lithium cations of the dimers. In both cases, THF binding to the lithium above or below the O_2Li_2 plane leads to diastereomeric species having central and planar chirality (Figure S15).[45] The relative position of the THF molecules is described by a prefix "*d/u*" added to the labels of the structures, to indicate that the THF molecule is on the side "down/up" of the O_2Li_2 plane. Interestingly, the most stable structure was found to be ***(d,u)*-D3a(THF)$_2$** resulting from the coordination to **D3a** of one THF molecule from the side down and the second one from side up of the O_2Li_2 core (viewed from left to right) (Fig 10 and S16). This structure is quite similar to that reported for **20** in the solid-state.[28] The metallacycles give rise to a ladder-type framework with the six-membered rings arranged anti with respect to the central O_2Li_2 four-membered ring. The latter is

slightly puckered (torsion angle O-Li-O-Li of 6.04º), whereas in **20** is essentially planar. The average O-Li distances of 1.947 Å fit very well with those measured in **20** (average: 1.964 Å).

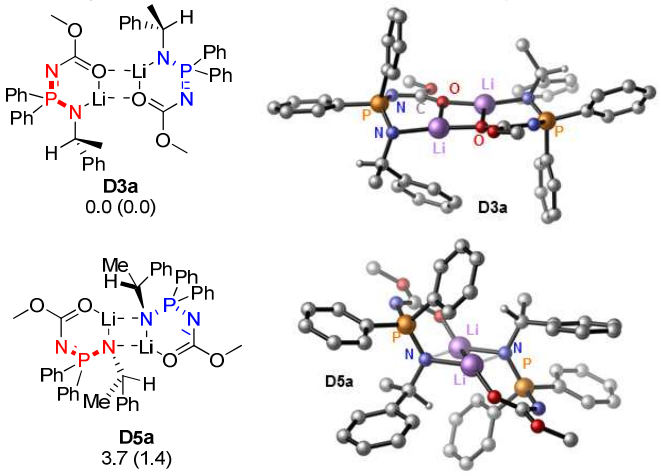

Figure 9. Favoured structures of unsolvated dimers **D3a** and **D5a**. Free energies and enthalpies (in parentheses) are given in kcal/mol with respect to **D3a**.

From the NMR spectroscopy point of view, isomers (*d,d*)-**D1a(THF)$_2$**, (*u,u*)-**D2a(THF)$_2$**, (*u,u*)-**D2a(THF)$_2$** and (*d,d*)-**D2a(THF)$_2$** are of C_2 symmetry and feature equivalent ^{31}P nuclei. However, the ^{31}P nuclei of (*d,u*)-**D3a(THF)$_2$**, and (*d,u*)-**D1a(THF)$_2$** are inequivalent and they will produce two signals of the same intensity in the ^{31}P NMR spectrum. These findings support the conclusions of the ^{31}P NMR in which dimers showing different ^{31}P signals were observed.

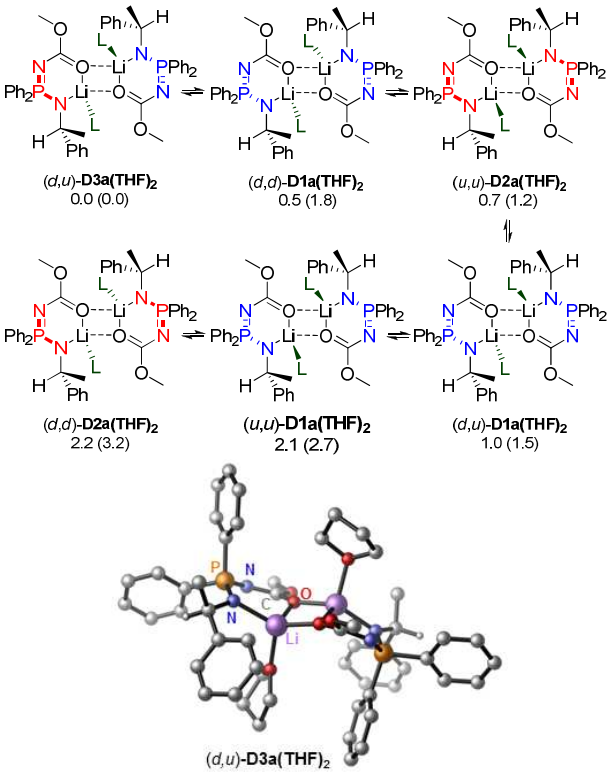

Figure 10. Possible exchange processes among the six most stable dissolvated dimers and 3D representation of (*d,u*)-**D3a(THF)$_2$**. Hydrogen atoms have been omitted for clarity.

Free energies and enthalpies (in parentheses) are given in kcal/mol with respect to (*d,u*)-**D3a(THF)$_2$**.

Compared with (*d,u*)-**D3a(THF)$_2$**, the most stable monomer **M2a(THF)$_2$** is destabilized by 4.2 kcal/mol, which suggest that only dimers should be detected in solution. This result is in agreement with the ΔG = 1.2 kcal/mol obtained from the log[D]-log[M] plot (Fig S10). However, it must be taken into account that formation of a dimer involves the equilibrium $2M(THF)_2 \leftrightarrows D(THF)_2 + 2THF$. Therefore, according to the Le Châtelier principle, in highly diluted samples the equilibirum would be shifted to the monomeric species. It is worthy of comment that the diastereoselectivity of the ortho-lithiation-electrophilic quench process shown in Scheme 1 remains unchanged in the range of concentration of 0.05 M to 0.3 M. This feature suggests that the *ortho*-lithiation proceeds through a monomer rather than a dimer.

Conclusions

In summary, we have carried out a detailed structural study of a *N*-lithiated phosphinimidic amide in solution and computationally. Multinuclear magnetic resonance experiments involving the nuclei ^{7}Li, ^{15}N and ^{31}P revealed that the ligand is coordinated to the lithium cation through the deprotonated nitrogen atom and the oxygen atom of the carbonyl group conjugated with the P=N linkage. The behaviour as an *O,N*-chelate ligand results in the formation of a six-membered ring. This feature is in striking contrast with the Li-N-P-N four-membered rings shown in the solid-state by all *N*-lithiated phosphinimidic amides reported to date. Importantly, based on NOE data obtained at -20 ºC it became apparent that the chiral auxiliary is spatially close to only one of the diastereotopic *P*-phenyl rings. This is a key aspect for understanding the highly diastereoselective *N,C$_{ortho}$*-dilithiation of phosphinimidic amides. Variable temperature and concentration NMR measurements evidenced the existence of complex monomer⇆dimer equilibria due to the participation of these species in additional dynamic processes.

The computational study provided deeper insight into the structure of the lithiated species. In the most stable monomers, the lithium atom is four-coordinated due to *O,N*-chelation by the ligand and additional binding to two THF molecules. These species might exist as isomers arising from two possible orientations of the methoxy group and two twist-boat conformations of the six-membered ring. Most probably, interconversion between the twist-boat conformers represents the dynamic process observed in the ^{1}H, ^{7}Li and ^{31}P NMR spectra measured at temperatures below -80 ºC. Furthermore, in these monomers, one *ortho*-proton of the *pro-S P*-phenyl ring is very close to the nitrogen atom of the $PNCO_2Me$ moiety, *i.e.*, in the right position for proton abstraction by a base, in agreement with the experimental results. Dimers are formed by connecting monomers through O-Li bridges with displacement of two THF molecules. The orientation of the THF molecules in the dimers determines the appearance of one or two signals in the ^{31}P-NMR spectrum. Significantly, the most stable dimer shows a ladder-type structure with the six-membered rings oriented anti with respect to the O_2Li_2 core and the THF molecules that complete the four-coordination of the lithium atoms are located on opposite sites of the O_2Li_2 plane. This structure is analogous to that found in the solid-state for the C_α-lithiated phosphazene **20**. Further work on the mechanism of diastereoselective ortho proton abstraction of *N*-lithiated phosphinimidic amide and on the structure of the *N,C$_{ortho}$*-dilithiated species is in progress.

Experimental

Materials and methods

All reactions and manipulations were carried out in a dry N_2 gas atmosphere using standard Schlenk procedures. THF and THF-d_8 were distilled from sodium/benzophenone immediately prior to use. *t*-BuLi was purchased from Sigma-Aldrich and was used as received. Low temperatures were always achieved with a N_2(l)/MeOH bath. Multinuclear magnetic resonance spectra were measured in a Bruker Avance 500 spectrometer (^{1}H, 500.13 MHz; ^{7}Li, 194.4 MHz; ^{13}C, 125.7 MHz; ^{15}N, 50.7 MHz; ^{31}P, 202.4 MHz) using a direct TBO ^{1}H/^{31}P/BB. The spectral references used were internal tetramethylsilane for ^{1}H and ^{13}C, $MeNO_2$ for ^{15}N, external 85% H_3PO_4 for ^{31}P, and 1 M LiBr in D_2O for ^{7}Li. A set of two complementary ^{31}P/^{7}Li-selective band pass/stop frequency filters was used for the measurement of NMR spectra involving ^{31}P and ^{7}Li nuclei. Standard Bruker software was used for acquisition and processing routines. Selected spectral parameters were as follows: ^{7}Li NMR (194.4 MHz): 24 *K* data points; spectral width 9690 Hz; exponential multiplication with a line broadening factor of 2 Hz. For resolution enhancement processing a Gaussian multiplication (GM) was applied to ^{7}Li (LB= –2, GB= 0.3). ^{31}P NMR (202.4 MHz): 128 *K* data points; spectral width 60606 Hz; exponential multiplication with a line broadening factor of 2 Hz. The ^{7}Li,^{31}P{^{1}H} HMQC 2D experiment was performed using spectral widths of 5399 Hz (^{31}P) and 2717 Hz (^{7}Li), a final matrix after zero filling of 1024×128 and an evolution delay of $^nJ_{PLi}$ 50 ms. The ^{7}Li,^{15}N HMQC 2D experiment was performed using spectral widths of 20271 Hz (^{15}N) and 2717 Hz (^{7}Li), a final matrix after zero filling of 1024×256 and an evolution delay of $^nJ_{NLi}$ 50 ms. The ^{31}P,^{15}N{^{1}H} HMQC 2D experiment was performed using spectral widths of 20271 Hz (^{15}N) and 5081 Hz (^{31}P), a final matrix after zero filling of 1024×128 and an evolution delay of $^nJ_{PN}$ 17 ms.

Computational Details

The geometries of all compounds were optimized with B3LYP[46] and a 6-31G(d) basis set in gas phase. At this level of calculation all stationary points were characterized as minimum and confirmed by vibrational analysis. Single point energy calculations were performed with the M06-2X[47] functional and a 6-311+G(d,p) basis set for other atoms. The SMD solvation model[37] was used in M06-2X single point energy calculations. THF was used as solvent. The reported free energies and enthalpies include zero-point energies and thermal corrections calculated at 183 K by B3LYP. All calculations were performed with Gaussian 09.[48] The 3D structures of molecules were generated using CYLView (http://www.cylview.org).

General procedure for the monolithiation of 13 and NMR sample preparation. To a solution of aminophosphazene **13** (0.4 mmol) in THF (5 mL) was added a solution of *t*-BuLi (0.23 mL of a 1.7 M solution in cyclohexane; 0.4 mmol; 1 eq) at -78 ºC. After 1 hour stirring, 0.5 mL of the reaction mixture were transferred to a 5 mm NMR tube under N_2 atmosphere placed into a refrigerated bath at the same temperature. Subsequently, the sample was transferred to the previously cooled magnet. Species **I** (average structure at -20 ºC): ^{1}H NMR (THF-d_8, 500.13 MHz) δ 1.32 (d, 3H, $^3J_{HH}$ 20 Hz, H-7), 3.68 (s, 3H, H-4), 4.22 (dc, 1H, $^3J_{HH}$ 20 Hz, $^3J_{HP}$ 6.4 Hz, H-6), 7.06 (t, 1H, $^3J_{HH}$ 7.3 Hz, H-11), 7.17 (t, $^3J_{HH}$ 7.3 Hz, H-10), 7.20 (m, H-14), 7.28 (t, $^3J_{HH}$ 7.1 Hz, H-15), 7.38 (m, H-14', H-15'), 7.44 (d, $^3J_{HH}$ 7.3 Hz, H-9), 7.66 (m, H-13), 7.79 (m, H-13') ppm. ^{13}C NMR (THF-d_8, 125.7 MHz) δ 28.64 (d, $^3J_{PC}$ 8.7 Hz, C-7), 55.35 (bs, C-6), 53.44 (bs, C-4), 124.81 (s, C-11), 126.50 (s, C-9), 127.03 (d, $^3J_{PC}$ 11.5 Hz, C-14), 127.32 (s, C-10), 127.48 (d, $^3J_{PC}$ 11.1 Hz, C-14'), 129.47 (s, C-15), 129.67 (s, C-15'), 132.07 (d, $^2J_{PC}$ 8.1 Hz, C-13), 132.29 (d, $^2J_{PC}$ 8.9 Hz, C-13'), 135.60 (d, $^1J_{PC}$ 109.9 Hz, C-12), 137.23 (d, $^1J_{PC}$ 117.8 Hz, C-12'), 151.53 (d, $^3J_{PC}$ 12.1 Hz, C-8), 164.09 (s, C-3) ppm. ^{31}P NMR (THF-d_8, 202.4 MHz) δ 19 ppm. ^{7}Li, NMR (THF-d_8, 194.4 MHz) δ 0.98 ppm. ^{15}N, NMR (THF-d_8, 50.7 MHz) δ -256.5 ($^1J_{PN}$ 16 Hz), -320.1 ($^1J_{PN}$ 36 Hz) ppm.

Acknowledgements

We thank the MICINN, MEC, MINECO and FEDER program for financial support (CTQ2011-27705). MC thanks MEC for a Ph.D. fellowship.

Notes and references

[a] Área de Química Orgánica, Universidad de Almería, Carretera de Sacramento s/n, 04120 Almería, Spain.

† Electronic Supplementary Information (ESI) available: 1D and 2D NMR spectra used in the structural assignment of species **I** in solution and Cartesian coordinates of all computed structures. See DOI: 10.1039/b000000x/

1 (*a*) F. Baier, Z. Fei, H. Gornitzka, A. Murso, S. Neufeld, M. Pfeiffer, I. Rudenauer, A. Steiner, T. Stey and D. Stalke, *J. Organomet. Chem.,* 2002, **661**, 111; (*b*) A. Steiner, S. Zacchini and P. I. Richards, *Coord. Chem. Rev.,* 2002, **227**, 193; (*c*) S. Collins, *Coord. Chem. Rev.* 2011, **255**, 118.

2 (*a*) U. Kilimann, M. Noltemeyer and F. T. Edelmann, *J. Organomet. Chem.,* 1993, **443**, 35; (*b*) A. Steiner and D. Stake, *Inorg. Chem.,* 1993, **32**, 1977; (*c*) R. Fleischer and D. Stalke, *Inorg. Chem.,* 1997, **36**, 2431; (*d*) B. Nekoueishahraki, H. W. Roesky, G. Schwab, D. Stern and D. Stalke, *Inorg. Chem.,* 2009, **48**, 9174.

3 (*a*) R. Boese, M. Düppmann, W. Kuchen and W. Peters, *Z. Anorg. Allg. Chem.,* 1998, **624**, 837; (*b*) B. F. Straub, F. Rominger and P. Hofmann, *Chem. Commun.,* 2000, 1611; (*c*) Y. V .Fedotova, A. N. Kornev, V. V. Sushev, Y. A. Kursky, T. G. Mushtina, N. P. Makarenko, G. K. Fukin, G. A. Abakumov, L. N. Zakharov and A. L. Rheingold, *J. Organomet. Chem.,* 2004, **689**, 3060; (*d*) R.Vollmerhaus, R. Tomaszewski, P. Shao, N. J. Taylor, K. J. Wiacek, S. P. Lewis, A. Al-Humydi and S. Collins, *Organometallics*, 2005, **24**, 494; (*e*) T. A. Peganova, A. V. Valyaeva, A. M. Kalsin, P. V. Petrovskii, A. O. Borissova, K. A. Lyssenko and N. A. Ustynyuk, *Organometallics,* 2009, **28***,* 3021; (*f*) A. Stasch, *Chem. Eur. J.,* 2012, **18**, 15105

4 (*a*) A. Recknagel, A. Steiner, M. Noltemeyer, S. Brooker, D. Stalke and F. T. Edelmann, *J. Organomet. Chem.,* 1991, **414**, 327; (*b*) H. Schumann, J. Winterfeld, H. Hemling, E. E. Hahn, P. Reich, K.-W. Brzezinka, F. T. Edelmann, U. Kilimann and R. Herbst-Irmer, *Chem.*

Ber., 1995, **128**, 395; (*c*) M. J. Sarsfield, M. Helliwell, J. Raftery, *Inorg. Chem.,* 2004, **43**, 3170; (*d*) A. N. Kornev, V. V. Sushev, Y. S. Panova, N. V. Belina, O. V. Lukoyanova, G. K. Fukin, S. Y. Ketkov, G. A. Abakumov, P. Lo□nnecke and E. Hey-Hawkins, *Inorg. Chem.,* 2012, **51**, 874.

5 (*a*) B. F. Straub and P. Hofmann, *Angew. Chem. Int. Ed.,* 2001, **40**, 1288; (*b*) B. F. Straub, I. Gruber, F. Rominger and P. Hofmann, *J. Organomet. Chem.,* 2003, **684**, 124; (*c*) P. Hofmann, I. V. Shishkov and F. Rominger, *Inorg. Chem.,* 2008, **47**, 11755; (*d*) I. V. Shishkov, F. Rominger and P. Hofmann, *Organometallics,* 2009, **28**, 1049.

6 (*a*) K. Albahily, S. Licciulli, S. Gambarotta, I. Korobkov, R. Chevalier, K. Schuhen and R. Duchateau, *Organometallics*, 2011, **30**, 3346; (*b*) K. Albahily, V. Fomitcheva, Y. Shaikh, E. Sebastiao, S. I. Gorelsky, S. Gambarotta, I. Korobkov and R. Duchateau, *Organometallics,* 2011, **30**, 4201; (*c*) K. Albahily, V. Formitcheva, S. Gambarotta, I. Korobkov, M. Murugesu and S. Gorelsky, *J. Am. Chem. Soc.,* 2011, **133**, 6380.

7 For recent references see: (*a*) R. L. Stapleton, J. Chai, N. J. Taylor and S. Collins, *Organometallics*, 2006, **25**, 2514; (*b*) C.-Y. Qi and Z.-X. Wang, *J. Polym. Sci. A,* 2006, **44**, 4621; (*c*) S. A. Ahmed, M. S. Hill, P. B. Hitchcock, S. F. Mansell and O. St John, *Organometallics*, 2007, **26**, 538; (*d*) S. Li, W. Miao, T. Tang, W. Dong, X. Zhang and D. Cui, *Organometallics*, 2008, **27**, 718; (*e*) S. Li, D. Cui, D. Li and Z. Hou, *Organometallics*, 2009, **28**, 4814; (*f*) Y. Yang, K. Lv, L. Wang, Y. Wang and D. Cui, *Chem. Commun*, 2010, **46**, 6150.

8 N. Nebra, C. Lescot, P. Dauban, S. Mallet-Ladeira, B. Martin-Vaca and D. Bourissou, *Eur. J. Org. Chem.,* 2013, 984.

9 W.-J. Guo and Z.-X. Wang, *J. Org.Chem.,* 2013, **78**, 1054.

10 V. V.Sushev, A. N. Kornev, Yu. A. Min'ko, N. V. Belina, Y. A. Kurskiy, O. V. Kuznetsova, G. K. Fukin, E. V. Baranov, V. K. Cherkasov and G. A. Abakumov, *J. Organomet. Chem.,* 2006, **691**, 879.

11 S. Wingerter, M. Pfeiffer, A. Murso, C. Lustig, T. Stey, V. Chandrasekhar, D. Stalke, *J. Am. Chem. Soc.,* 2001, **123**, 1381

12 A. Malassa, B. Schulze, B. Stein-Schaller, H. Görls, B. Weber and M. Westerhausen, *Eur. J. Inorg. Chem,* 2011, 1584.

13 H. Ackermann, O. Bock, U.Müller and K. Dehnicke, *Z. Anorg. Allg. Chem.,* 2000, **626**, 1854.

14 For related structures of NPN vanadium complexes see: (*a*) M. Witt, H. W. Roesky, M. Noltemeyer, G. M. Sheldrick, *Angew. Chem., Int. Ed. Engl.* 1988, **27**, 250; (*b*) P. Olms, H. W. Roesky, K. Keller, M. Noltemeyer, R. Bohra, H.-G. Schmidt and D. Stalke, *Chem. Ber.,* 1991, **124**, 2655.

15 (*a*) Complex **7**: see references 2b and 4a; (*b*) complex **8**: E. Muller, J. Muller, H.-G. Schmidt, M. Noltemeyer and F. T. Edelmann, *Phosphorus, Sulfur, Silicon, Relat. Elem.,* 1996, **1**, 121; (*c*) complex **9**: M. Schultz, B. F. Straub and P. Hofmann, *Acta Crystallogr., Sect. C,* 2002, **C58**, m256; (*d*) complex **10**: A. J. Edwards and E. Wenger, *Aust. J. Chem.,* 2002, **55**, 249; (*e*) complex **11**: see reference 4d.

16 (*a*) J. García-López, I. Fernández, M. Serrano-Ruiz and F. López-Ortiz, *Chem. Commun.,* 2007, 4674; (*b*) P. Oña-Burgos, I. Fernández, L. Roces, L. Torre-Fernández, S. García-Granda and F. López-Ortiz, *Organometallics,* 2009, **28**, 1739; (*c*) J. García-López, V. Yáñez-Rodríguez, L. Roces, S. García-Granda, A. Martínez, A. Guevara-García, G. R. Castro, F. Jiménez-Villacorta, M. J. Iglesias and F. López-Ortiz, *J. Am. Chem. Soc.,* 2010, **132**, 10665; (*d*) C. Popovici, P. Oña-Burgos, I. Fernández, L. Roces, S. García-Granda, M. J. Iglesias and F. López-Ortiz, *Org. Lett.,* 2010, **12**, 428; (*e*) C. Popovici, I. Fernández, P. Oña-Burgos, L. Roces, S. García-Granda and F. López-Ortiz, *Dalton Trans.,* 2011, **40**, 6691; (*f*) H. el Hajjouji, E. Belmonte, J. García-López, I. Fernández, M. J. Iglesias, L. Roces, S. García-Granda, A. El Laghdach and F. López-Ortiz, *Org. Biomol. Chem.*, 2012, **10**, 5647; (*g*) V. Yáñez-Rodríguez, M. Á. del Águila, M. J. Iglesias, F. López-Ortiz, *Tetrahedron*, 2012, **68**, 7355.

17 M. Casimiro, L. Roces, S. García-Granda, M. J. Iglesias and F. López-Ortiz, *Org. Lett.,* 2013, **15**, 2378.

18 For directed ortho lithiation of phosphazenes see: (*a*) C. G. Stuckwisch, *J. Org. Chem.* 1976*,* **41**, 1173; (*b*) A. Steiner and D. Stalke, *Angew. Chem., Int. Ed. Engl.,* 1995, **34**, 1752; (c) D. Aguilar, I. Fernández, L. Cuesta, V. Yañez-Rodríguez, T. Soler, R. Navarro, E. P. Urriolabeitia and F. López-Ortiz, *J. Org. Chem*., 2010, **75**, 6452; (*d*) E. Martinez-Arripe, F. Jean-Baptiste-dit-Dominique, A. Auffrant, X.-F. Le Goff, J. Thuilliez and F. Nief, *Organometallics,* 2012, **31**, 4854; (*e*) Q. Zhang, X.-Q. Zhang and Z.-X. Wang, *Dalton Trans*., 2012, **41**, 10453.

19 For recent reviews on the applications of *P*-chiral in asymmetric synthesis see: (*a*) S. E. Denmark and J. Fu, *Chem. Rev.,* 2003, **103**, 2763; (*b*) Y. Wei and M. Shi, *Acc. Chem. Res.,* 2010, **43**, 1005; (*c*) *Phosphorus Ligands in Asymmetric Catalysis*, ed. A. Börner, Wiley-VCH, Weinheim, 2008; (*d*) V. A. Pavlov, *Tetrahedron* 2008, **64**, 1147; (*e*) T. Nemoto, *Chem. Pharm. Bull.,* 2008, **56**, 1213; (*f*) S. Lühr, J. Holz and A. Börner, *ChemCatChem*, 2011, **3**, 1708; (*g*) *P-Chiral Ligands in Phosphorus(III) Ligands in Homogeneous Catalysis: Design and Synthesis*, ed. P. C. J. Kamer and P. W. N. M. van Leeuwen, Wiley, Chichester, U.K., 2012.

20 H. Schmidbaur, K. Schwirten and H. Pickel, *Chem. Ber.,* 1969, **102**, 564.

21 O. J. Scherer and G.Schieder, *J. Organomet. Chem.,* 1969, **19**, 315.

22 Exclusive ortho monolithiation has been reported for a phosphinimidic amide analogous to **13**. See reference 18e

23 F. López-Ortiz and R. J. Carbajo, *Curr. Org. Chem.,* 1998, **2**, 97.

24 (*a*) F. López-Ortiz, E. Peláez-Arango and P. Gómez-Elipe, *J. Magn. Res.,* 1996, **119**, 247; (*b*) E. Peláez-Arango, F. J. García-Alonso, G. Carriedo and F. López-Ortiz, *J. Magn. Res.,* 1996, **121**, 154; (*c*) G. Carriedo, F. J. García-Alonso, J. L. García, R. J. Carbajo and F. López-Ortiz, *Eur. J. Inorg. Chem.,* 1999, 1015; (*d*) R. J. Carbajo and F. López-Ortiz, *J. Magn. Res.,* 2001, **148**, 165;

25 Chemical shift differences arising from solvent effects ($CDCl_3$ *vs* THF-d_8) are assumed to be of little significance.

26 I. Fernández, P. Oña-Burgos, F. Armbruster, I. Krummenacher and F. Breher, *Chem. Commun.,* 2009, 2586.

27 Coordination via extended conjugation has been observed in the Cu(II) complex of a *N,N'*-bis(cyanamido)phosphinimidic amide. M. Taillefer, N. Inguimbert, L. Jäger, K. Merzweiler and H. Cristau, *Chem. Commun.,* 1999, 565

28 I. Fernández, J. M. Álvarez-Gutiérrez, N. Kocher, D. Leusser, D. Stalke, J. González and F. López-Ortiz, *J. Am. Chem. Soc.,* 2004, **124**, 15184.

29 Recent reviews: (*a*) D. Li, I. Keresztes, R. Hopson and P. G. Williard, *Acc. Chem. Res*., 2009, **42**, 270; (*b*) V. H. Gessner, C. Daeschlein and C. Strohmann, *Chem. Eur. J.,* 2009, **15**, 3320; (*c*) A. Harrison-Marchand, H. Gerard and J. Maddaluno, *New J. Chem.,* 2012, **36**, 2441; (*d*) H. J. Reich, *Chem. Rev.,* 2013, **113**, 7130; (*e*) R. E. Mulvey and S. D. Robertson, *Angew. Chem., Int. Ed.,* 2013, **52**, 11470.

30 (*a*) K. -M. Marstokk and H. Møllendal, *Acta Chem. Scand.,* 1999, **53**, 79; (*b*) D. Kaur, P. Sharma and P. V. Bharatam*, J. Mol. Struct. (Theochem),* 2005, **757**, 149.

31 A very similar value is obtained when the concentration of species **Mγ** and **Mδ** is included in the total concentration of monomeric species (Fig S11).
32 T. Fox, H. Hausmann and H. Günther, *Magn. Reson. Chem*., 2004, **42**, 788.
33 I. Fernández, M. G. Davidson, R. D. Price and F. López-Ortiz, *Dalton Trans.,* 2009, 2438.
34 I. Fernández and F. López-Ortiz, *Chem. Commun.* **2004**, 1142.
35 Lithium azaenolates also exist in the solid-state as aggregates involving Li_2O_2 cores, rather than N-Li-N bridges. (*a*) T. Maetzke, C. P. Hidber and D. Seebach, *J. Am. Chem. Soc.,* 1990, **112**, 8248; (*b*) T. Maetzke and D. Seebach, *Organometallics*, 1990, **9**, 3032; (*c*) S. R. Boss, R. Haigh, D. J. Linton, P. Schooler, G. P. Shields and A. E. H. Wheatley, *Dalton Trans.,* 2003, 1001.
36 I. Fernández, P. Oña-Burgos, J. M. Oliva and F. López-Ortiz, *J. Am. Chem. Soc.,* 2010, **132**, 5193.
37 A. V. Marenich, C. J. Cramer and D. G. Truhlar, *J. Phys. Chem. B,* 2009, **113**, 6378
38 T. Stey and D, Stalke in *The Chemistry of Organolithium Compounds*, Z. Rappoport and I. Marek, Eds., Wiley: New York, 2004, Vol. 1, Chap. 2, pp 47-120.
39 For simplicity, we have used a color code associated to the relative position of the P atom with respect to the CH-N-Li plane: blue and red for the position below and above that plane, respectively. The reason for the different labelling schemes between NMR and theoretical studies is that the species identified in each study can't be correlated unequivocally.
40 (*a*) A. Wu and D.Cremer, *Int. J. Mol. Sci.,* 2003, **4**, 158; (*b*) A. V. Chertkov, O. I. Pokrovskiy, A. K. Shestakova and V. A. Chertkov, *Chem. Heterocyc. Comp.,* 2008, **44**, 621; (*c*) P. Duffy, J. A. Sordo and F. Wang, *J. Chem. Phys.,* 2008, **128**, 125102.
41 S. Wingerter, M. Pfeiffer, A. Murso, C. Lustig, T. Stey, V. Chandrasekhar and D. Stalke, *J. Am. Chem. Soc.,* 2001, **123**,1381.
42 The limiting value for a tetrahedral configuration is of 0.71. U. Kolb, M. Dräge and B. Jousseaume, *Organometallics*, 1991,**10**, 2737.
43 (*a*) P. R. Rablen, *J. Org. Chem.,* 2000, **65**, 7930; (*b*) E. A. Basso and R. M. Pontes, *J. Mol. Struct. (Theochem)*, 2002, **594**, 199; (*c*) M. J. Deetz, C. C. Forbes, M. Jonas, J. P. Malerich, B. D. Smith and O. Weist, *J. Org. Chem.,* 2002, **67**, 3949; (*d*) A. R. Modaressi-Alam, P. Najafi, M. Rostamizadeh, H. Keykha, H.-R. Bijanzadeh and E. Kleinpeter, *J. Org. Chem.,* 2007, **72**, 2208; (*e*) F. S. Grasel, T. Charao De Oliveira, L. A. M. Fontoura, I. J. C. Rigotti and P. A.Netz, *Int. J. Quantum Chem.,* 2012, **112**, 1678.
44 CIPE: Complex Induced Proximity Effect. Reviews: (*a*) P. Beak and A. I. Meyers, *Acc. Chem. Res*., 1986, **19**, 356; (*b*) P. Beak, A. Basu, D. J. Gallagher, Y. S. Park and S. Thayumanavan, *Acc. Chem. Res.,* 1996, **29**, 552; (*c*) A. Basu and S. Thayumanavan, *Angew. Chem. Int. Ed.,* 2002, **41**, 716; (*d*) M. C. Whisler, S. MacNeil, V. Snieckus and P. Beak, *Angew. Chem., Int. Ed.,* 2004, **43**, 2206; (*e*) D. Tilly, J. Magolan and J. Mortier, *Chem. Eur. J.,* 2012, **18**, 3804.
45 K. Fuji and T. Kawabata, *Chem. Eur. J.,* 1998, **4**, 373.
46 (*a*) A. D. Becke, *J. Chem. Phys.,* 1993, **98**, 5648; (*b*) C. Lee, W. Yang and R. G. Parr, *Phys. Rev. B,* 1988, **37**, 785.
47 Y. Zhao and D. G. Truhlar, *Theor. Chem. Acc.,* 2008, **120**, 215.
48 Gaussian 09, Revision B.01, M. J. Frisch, G. W. Trucks, H. B. Schlegel, G. E. Scuseria, M. A. Robb, J. R. Cheeseman, G. Scalmani, V. Barone, B. Mennucci, G. A. Petersson, H. Nakatsuji, M. Caricato, X. Li, H. P. Hratchian, A. F. Izmaylov, J. Bloino, G. Zheng, J. L. Sonnenberg, M. Hada, M. Ehara, K. Toyota, R. Fukuda, J. Hasegawa, M. Ishida, T. Nakajima, Y. Honda, O. Kitao, H. Nakai, T. Vreven, J. A. Montgomery, Jr., J. E. Peralta, F. Ogliaro, M. Bearpark, J. J. Heyd, E. Brothers, K. N. Kudin, V. N. Staroverov, T. Keith, R. Kobayashi, J. Normand, K. Raghavachari, A. Rendell, J. C. Burant, S. S. Iyengar, J. Tomasi, M. Cossi, N. Rega, J. M. Millam, M. Klene, J. E. Knox, J. B. Cross, V. Bakken, C. Adamo, J. Jaramillo, R. Gomperts, R. E. Stratmann, O. Yazyev, A. J. Austin, R. Cammi, C. Pomelli, J. W. Ochterski, R. L. Martin, K. Morokuma, V. G. Zakrzewski, G. A. Voth, P. Salvador, J. J. Dannenberg, S. Dapprich, A. D. Daniels, O. Farkas, J. B. Foresman, J. V. Ortiz, J. Cioslowski, and D. J. Fox, Gaussian, Inc., Wallingford CT, 2010.

Graphical Content Entry

The origin of the diastereoselective N,Cortho-dilithiation of (R)-Ph2P(=NCO2Me)NHCH(Me)Ph has been established based on a multinuclear magnetic resonance and computational structural study of the N-monolithiated species.